Silicon Bulk Mobility at High Ambient Temperatures

Andreas Schenk [1]

Technical Report No. 99/22

[1] **This work was supported by the German Bundesministerium für Bildung und Forschung under contract 01 M 3034 A. The authors are responsible for the contents of this publication.**

Abstract

One of the goals of the PARASITICS project was the evaluation of decisive physical models in the high temperature range (300 K – 700 K) by comparison between simulation and electrical measurements of suitable test structures. Various van der Pauw devices were examined to test the microscopic-based mobility model of Schenk [1]. In order to make the comparison complete, calculated Hall factors as function of temperature and doping were adopted instead of using constant values. In the case of holes both the magnitude and the temperature slope are in reasonable agreement with the Hall data corrected by the Hall factors. All n-type samples showed the tendency of a temperature slope that is too steep when compared with the mobility model. Contradictions with well accepted literature data were found for a moderately doped n-type device, where the density was reliable and did not change with temperature up to 520 K. For all other samples the measured total density increased with temperature indicating strong thermal pn-leakage. The latter is believed to falsify the temperature slope of the mobility. Because of the sophisticated test structures with very inhomogeneous doping profiles and the observed thermal pn-leakage, a re-assessment of the mobility model [1] and its parameters based on the high-temperature Hall data obtained in the PARASITICS project was not taken to be advisable.

1 Test devices for high-temperature Hall data

The list of evaluated van der Pauw structures is shown in Table 1. The numbers in the second column are the process-simulated peak concentrations of the first profile underneath the surface. The third column contains the measured average densities at 300 K ($n + p$). In some cases both values differ considerably. The usefulness

Table 1: Van der Pauw structures used in this work. Second column: simulated maxima of the doping profiles underneath the surface, third column: average carrier density at 300 K obtained during the Hall measurements.

device	sim. peak doping	meas. $n + p$ at 300 K
NW_PY1_CI	$2 \times 10^{16}\,\mathrm{cm}^{-3}$	$1.8 \times 10^{16}\,\mathrm{cm}^{-3}$
NEE_	$2.45 \times 10^{19}\,\mathrm{cm}^{-3}$	$7.79 \times 10^{18}\,\mathrm{cm}^{-3}$
NP_	$1.37 \times 10^{20}\,\mathrm{cm}^{-3}$	$1.61 \times 10^{20}\,\mathrm{cm}^{-3}$
PF_PW_PY	$6 \times 10^{16}\,\mathrm{cm}^{-3}$	$4.34 \times 10^{16}\,\mathrm{cm}^{-3}$
PB_MTL1_CI	$2 \times 10^{17}\,\mathrm{cm}^{-3}$	$2.15 \times 10^{17}\,\mathrm{cm}^{-3}$
PP_MTL1_CI	$8 \times 10^{19}\,\mathrm{cm}^{-3}$	$7.74 \times 10^{19}\,\mathrm{cm}^{-3}$

of these test devices for Hall measurements is restricted because of two reasons. Firstly, the doping profiles are very inhomogeneous. Secondly, the presence of a pn-junction causes strong thermal leakage and a spreading of the current when the temperature exceeds a certain value. This turns the conductivity from monopolar into bipolar before the intrinsic regime is reached. An example are the symbols of device NW_PY1_CI (see Fig. 6, n = $1.8 \times 10^{16}\mathrm{cm}^{-3}$). Squares are the data obtained with floating pn-junction, circles are the data with biased epi- and body-contacts such that the thermal barrier of the pn-junction was increased to repel holes up to 650 K. However, in most cases the measured total density $n + p$ monotonously increased with temperature, starting already at room temperature.

A cross section and the simulated doping profile along a vertical cut of a typical device are shown in Fig. 1. The right-most contact belongs to the van der Pauw structure, the middle and the left contacts are the body- and epi-contacts, respectively.

2 Hall factors

Hall mobility and conductivity mobility are related by the Hall factor: $\mu_H = r_H \mu$. The Hall factor $r_H = \langle\tau^2\rangle/\langle\tau\rangle^2$ depends on the total microscopic momentum relaxation time τ. Therefore, it is a function of impurity concentration and temperature. The Hall factors for electrons and holes as function of temperature were calculated by Dr. Christoph Jungemann (Uni Bremen) using their Monte Carlo program. Coulomb scattering was treated with the help of the microscopic relaxation time. The doping levels correspond to the simulated peak concentrations of the evaluated van der Pauw resistors. As shown in Fig. 2, the temperature dependence of the Hall factor strongly depends on the doping level. In the case of electrons a monotonous increase of r_H

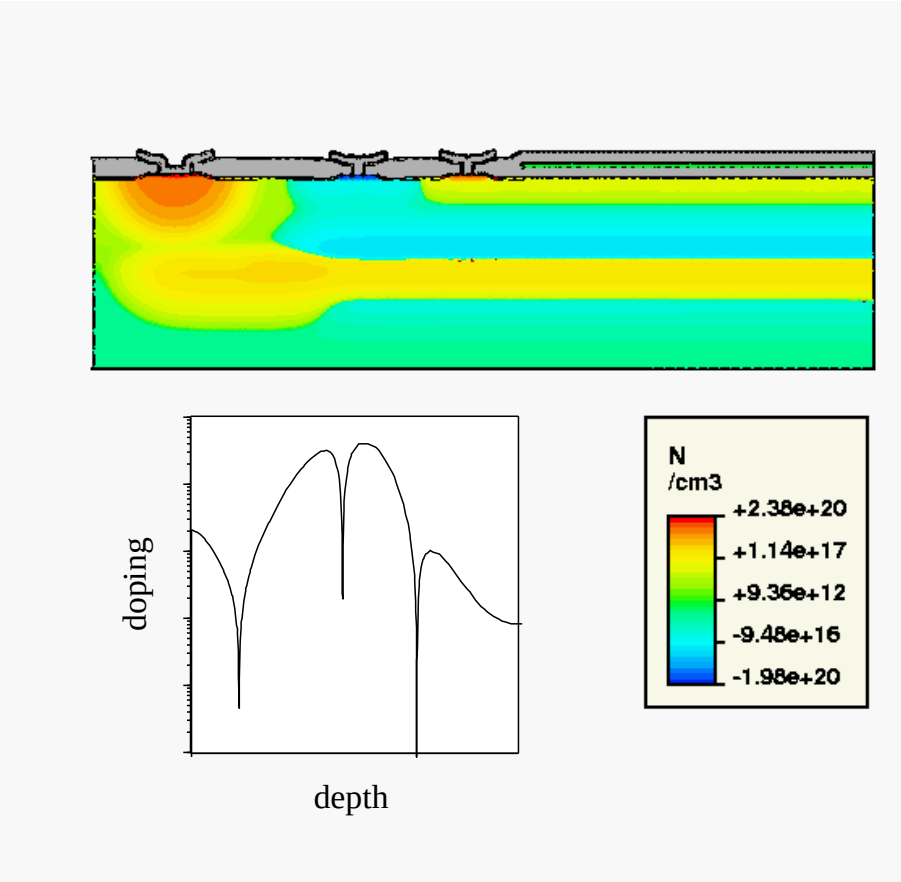

Figure 1: Cross section of the device NW_PY1_CI and doping profile along a vertical cut.

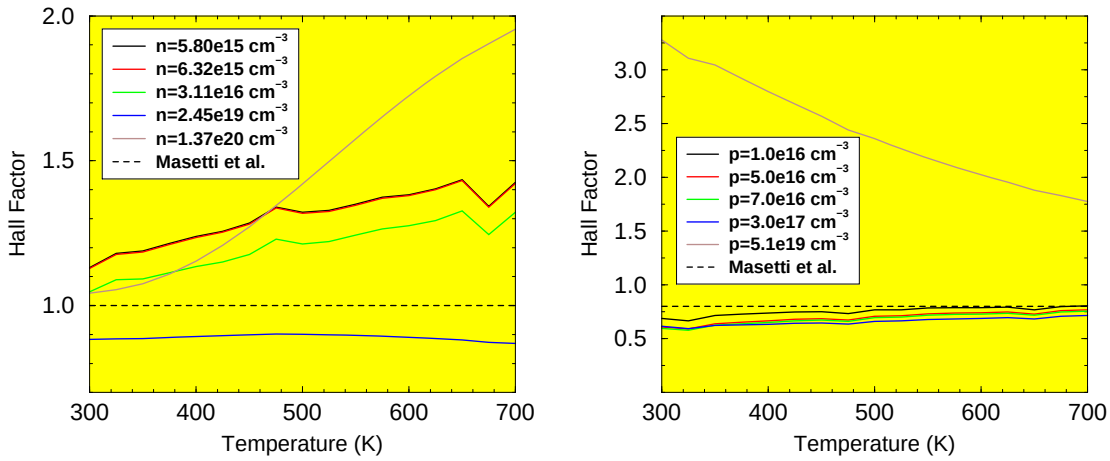

Figure 2: Calculated Hall factors for electrons (left) and holes (right) as function of temperature for various doping densities. The dashed lines are the constant values used by Masetti et al. in interpreting their Hall data.

was found for moderate doping, an almost constant value of 0.9 for $\approx 2 \times 10^{19}$ cm^{-3}, and a strong increase in the heavy doping range. The often used value 1 (dashed line) can only be regarded as a crude average at 300 K. In the case of holes r_H approaches

the often used value 0.8 at high temperatures for moderate doping. A large and monotonously decreasing function was found for $\approx 5 \times 10^{19}$ cm^{-3}.

In the further analysis all Hall mobility data were transformed with the corresponding Hall factors $r_H(T_L, N_{imp})$ from Fig. 2 regardless of a possible deviation from the true values, especially at the highest doping levels.

3 Temperature dependence of the Ohmic drift mobility models [1] and [2] at different doping levels

Details of the microscopic-based bulk mobility model of Schenk can be found in Refs. [1] and [3]. Deformation-potential constants and phonon frequencies are similar to those used in first-principle Monte Carlo codes and were adjusted in form of "effective" values by comparison with experimental data. The explicit expression reads in the case of electrons

$$\mu_n\left(T_L, T_n, N_{imp}\right) = \frac{\mu_n^{(0)}(T_L)}{f_{ac}(T_L, T_n) + f_{int}(T_L, T_n) + f_{imp}\left(T_L, T_n, N_{imp}\right)}$$

where $\mu_n^{(0)}$ is a "scaling" mobility

$$\mu_n^{(0)}(T_L) = \frac{9\,q\hbar}{m_{dn}\,k_B T_L} = 403.8\left(\frac{300}{T_L}\right)\left(\frac{m_0}{m_{dn}}\right)\frac{cm^2}{Vs}$$

which gives $1199\,cm^2/Vs$ at room temperature. The terms in the denominator contain the effects of acoustic-phonon scattering (ac), inter-valley-phonon scattering (int), and ionized impurity scattering (imp):

$$f_{ac} = 3.53 \times 10^{-4}\left(\frac{m_{dn}}{m_0}\right)^{5/2}\sqrt{\frac{300}{T_n}}\sqrt{1+24\tilde{\alpha}}\sum_{j=LA,TA}\frac{D_j^2}{x_j}e^{-x_j}\left(1+\sqrt{8x_j}\sqrt{1+8\tilde{\alpha}}\right)\,,$$

$$f_{int} = 1.34 \times 10^{-19}\frac{D_{int,n}^2}{\hbar\omega_{int,n}}\sqrt{\frac{T_n}{300}}\left(\frac{m_{dn}}{m_0}\right)^{\frac{3}{2}}\left(\frac{300}{T_L}\right)\sqrt{1+24\tilde{\alpha}}\,\sinh^{-1}(\xi)\xi^2 K_2(\xi)\,,$$

$$f_{imp} = f_{n,0}\,5.88 \times 10^{-19} N_{imp}\sqrt{\frac{m_0}{m_{dn}}}\left(\frac{300}{T_n}\right)^{\frac{3}{2}}\left(\frac{300}{T_L}\right)\{[(a_n+1)E_1(a_n)e^{a_n}-1]\times$$

$$\times(1-4\tilde{\alpha}a_n)+4\tilde{\alpha}E_1(a_n)e^{a_n}\}\,,$$

where

$$x_j = \frac{m_{dn}c_j^2}{2k_B T_n}, \quad \xi = \frac{\hbar\omega_{int,n}}{2k_B T_n}, \quad \tilde{\alpha} = \alpha k_B T_n\,.$$

The dispersive screening parameter a_n itself is a strong function of both the carrier density and the temperature

$$a_n = \frac{\pi\hbar^2 q^2 Z}{2 m_{dn}(T_L)\epsilon_s} \frac{J(\hat{q},\alpha)}{(k_B T_n)^2} \frac{\partial n}{\partial \eta_n} \ .$$

The dependence on lattice temperature T_L originates from the phonon occupation numbers, the dependence on the carrier temperature T_n from the electron distribution function. In the Ohmic regime T_n=T_L (thermalized carriers). The only "fudge" factor is $f_{n,0}$ which compensates for the breakdown of the Born approximation (first-order perturbation theory). At room temperature, $f_{n,0} = 2.3$ yields a good fit to the experimental data of Masetti et al. [4] up to a concentration of 10^{19} cm^{-3}. Since the Born approximation becomes increasingly valid with rising temperature, $f_{n,0}$ is actually a function of temperature and should asymptotically approach unity.

The DESSIS$_{-\mathrm{ISE}}$ default model [2] is a fit to the measured doping dependence (Masetti et al. [4]) at **room temperature**, combined with a fit for the T_L-dependence of the "lattice" mobility measured under **low-doping conditions**:

$$\mu_n(T, N_{imp}) = \mu_{min} + \frac{\mu_L \left(\frac{T}{300}\right)^{-2.5} - \mu_{min}}{1 + (N_{imp}/N_{ref,1})^{\alpha}} - \frac{\mu_1}{1 + (N_{ref,2}/N_{imp})^{\beta}} \ .$$

Hence, it is only correct in two one-dimensional sub-spaces of the full two-dimensional parameter space $\{T_L, N_{imp}\}$, namely for $\{300\,\mathrm{K}, N_{imp}\}$ and $\{T_L, 0\}$ (see below).

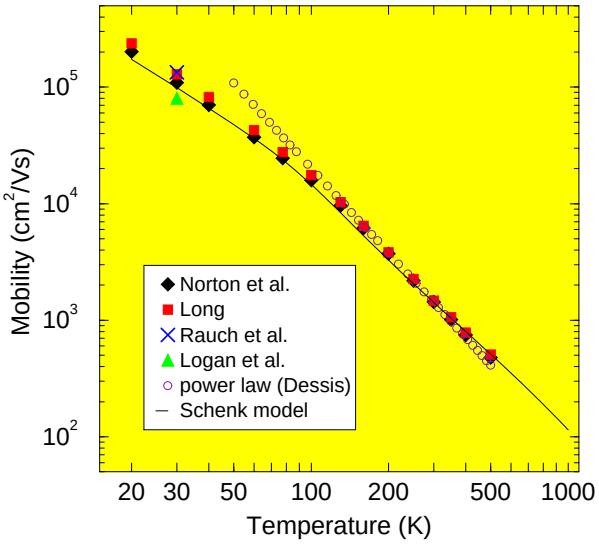

Figure 3: Electron bulk mobility as function of lattice temperature as it turns out from Schenk's model compared to experimental data and the DESSIS$_{-\mathrm{ISE}}$ default model [2].

In Fig. 3 both mobility models as a function of T_L for negligible doping (i.e. in the parameter sub-space $\{T_L, 0\}$) are compared with experimental data from the literature. The coincidence is equally good, although the power -2.5 obviously overestimates the drop.

Fig. 4 shows the partial "imp"-mobilities for frozen lattice, i.e. setting f_{ac} and f_{int} equal to zero in the above formula for $\mu_n\left(T_L, T_n, N_{imp}\right)$, over the whole temper-

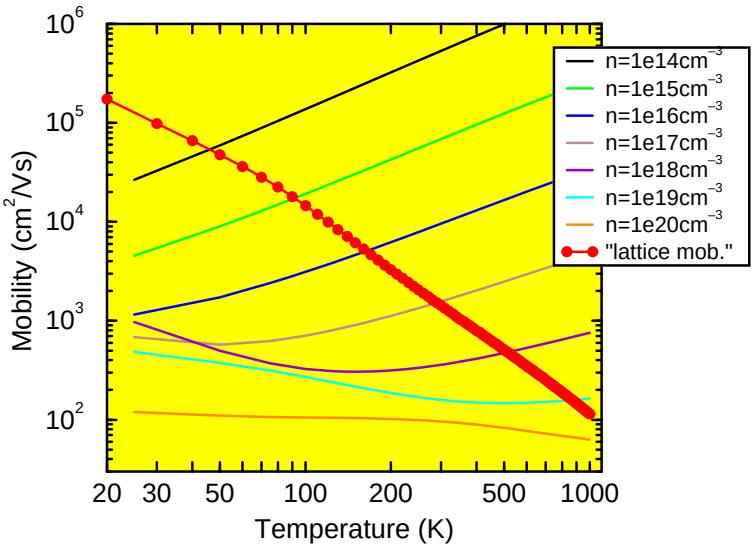

Figure 4: Partial "imp"-mobilities (frozen lattice) as function of temperature for various doping levels. The red curve with circles is the phonon-limited mobility (negligible doping).

ature range with the density (doping) as family parameter. The temperature dependence originates from the complicated function $f_{imp}\left(T_n = T_L, N_{imp}\right)$ and is hard to predict by a simple analytical function, especially at high doping levels. In the temperature range between 300 K and 1000 K one finds a monotonous increase up to densities of a few times 10^{18} cm^{-3} with a slope that strongly increases with decreasing doping. This behavior can be explained by the increasing average thermal velocity and, therefore, the reduced impact of the Coulomb scattering on the average drift velocity. In the heavy doping range the "imp"-mobility slightly decreases with temperature due to degeneracy effects and reduced screening (note that $a_n \sim T^{-2}$).

For comparison the phonon-limited mobility (negligible doping) is shown as red curve with circles in Fig. 4. For each decade of the density there is a cross-over between dominance of impurity scattering and dominance of phonon scattering at a particular temperature. The resulting total mobilities are shown in the left part of Fig. 5. One can see that for low and intermediate doping all curves converge to the phonon-limited mobility at high temperatures. Only in the heavy doping regime impurity scattering remains dominant. The corresponding behavior of the fit mobility model [2] is depicted in the right part of Fig. 5. Agreement can only be expected at

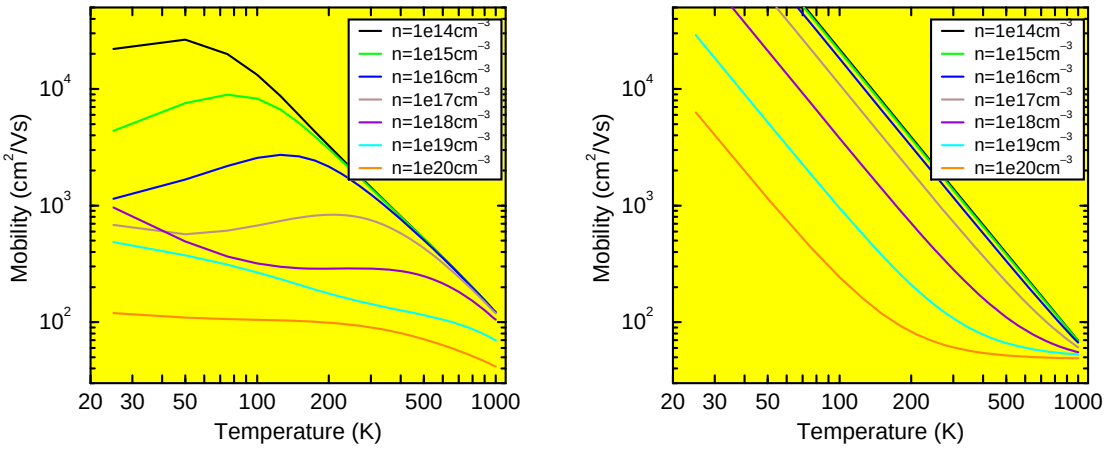

Figure 5: Total mobilities as function of temperature for various doping levels. Left: Schenk's model [1], right: DESSIS$_{-\mathrm{ISE}}$ default model [2].

300 K as discussed above. Moreover, the "high-temperature limit" turns out from fit parameters of the **doping** dependence!

4 Comparison with measurements

Measured and simulated mobilities in the temperature range between 300 K and 700 K are presented in Figs. 6 and 7, where only the usable test devices listed in Table 1 have been included. For a fair comparison, both a log-lin and a log-log plot are shown. The mobilities for the measured densities at 300 K were included as dashed curves (compare Table 1) in all cases of a large difference between simulated and measured concentrations. The green diamonds in Fig. 6 represent the low-doping (phonon-limited) mobility from Fig. 3. It merges with the curve for $\mathrm{n} = 1.8 \times 10^{16}$ cm^{-3} at about 500 K, as already stated above. The blue diamonds in Fig. 7 are the uncorrected Hall data for $\mathrm{p} = 2 \times 10^{17}$ cm^{-3} which highlight the strong influence of the Hall factor.

5 Discussion

The agreement is generally better for holes than for electrons. In the former case both the magnitude and the temperature slope are in reasonable agreement with the drift mobility data (Hall data corrected by the Hall factor). The misfit for PB_MTL1_CI (2×10^{17}) between 300 K and 400 K could also be due to an underestimation of the Hall factor in this temperature range. The almost constant slope of the heavily doped sample PP_MTL1_CI (8×10^{19}cm^{-3}) is well reproduced, but the simulated drift mobility turns out to be two times too large. Again, the surprisingly large Hall factor (3.25 – 1.75) may considerably contribute to this deviation.

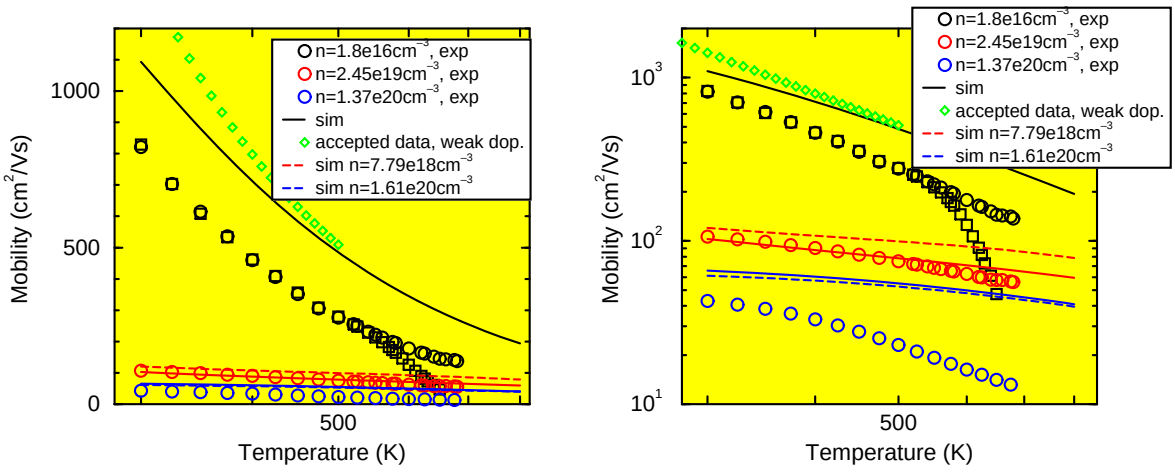

Figure 6: Electron bulk mobility in the temperature range between 300 K and 700 K. Comparison between measured drift mobility (Hall data corrected by Hall factor as described in the text) and Schenk's model (solid lines). Left: log-lin plot, right: log-log plot.

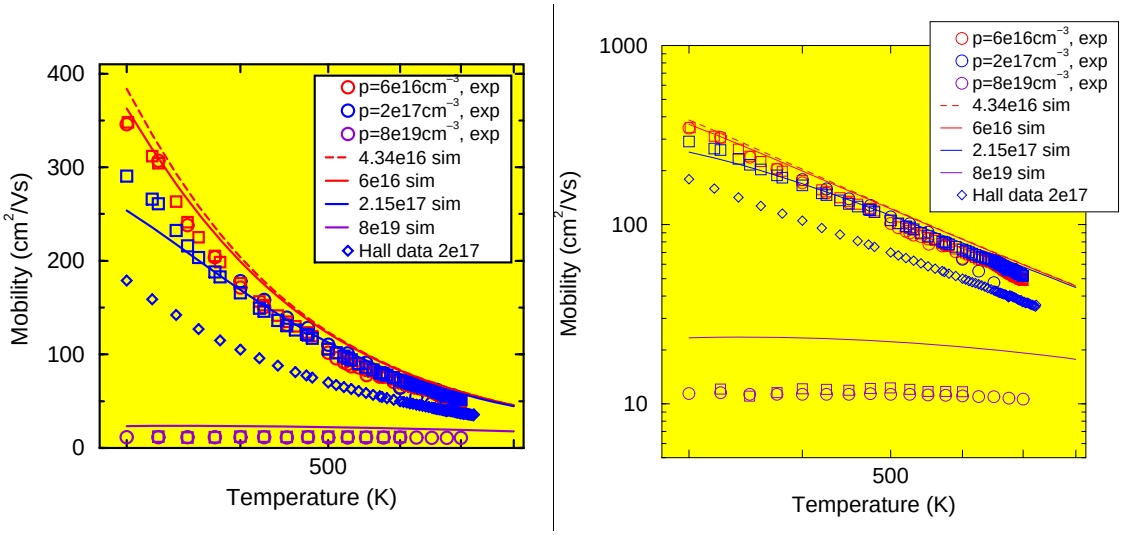

Figure 7: Hole bulk mobility in the temperature range between 300 K and 700 K. Comparison between measured drift mobility (Hall data corrected by Hall factor as described in the text) and Schenk's model (solid lines). Left: log-lin plot, right: log-log plot.

In the case of electrons the log-log plot reveals that only the data of sample NEE_ with $n = 2.45 \times 10^{19}\,\mathrm{cm}^{-3}$ are well reproduced. Using the measured average density here, however, would result in a temperature slope which is also too weak, as it is

observed as a general tendency for all n-type samples. It is worthwhile to discuss sample NW_PY1_CI ($1.8 \times 10^{16}\,\mathrm{cm}^{-3}$) in more detail. At 300 K the misfit amounts about 30 % which cannot be explained by the Hall factor. For comparison, in Fig. 6 the well accepted data for negligible doping are shown (green diamonds) which approach the theoretical curve (solid black) at 500 K. Here the misfit is already 75 %. Since for higher T the mobility is solely determined by phonon scattering, the slope of the theoretical curve reflects the T-dependence of $\mathrm{f_{ac}}$ and $\mathrm{f_{int}}$. The latter is based on two assumptions: the distribution function is Maxwellian-like and the band structure is nearly parabolic. Both assumptions are more than reasonable for thermalized carriers at 500 K lattice temperature. Using a constant Hall factor equal to 1 would only slightly improve the picture. Hence the measured data are not reliable in the sense that they represent the electron drift mobility and do not justify modifications of the mobility formula to enforce a better fit. The strong slope of the heavily doped sample NP_ ($1.37 \times 10^{20}\,\mathrm{cm}^{-3}$) is caused by the rapidly increasing Hall factor (compare Fig. 2). The 50 % deviation at 300 K is probably the result of the simplified model for impurity scattering (Born approximation, no clustering effects).

In conclusion, no re-assessment of the mobility model of Schenk is indicated by the high-temperature Hall data obtained in the PARASITICS project. The main reason is given by the sophisticated test structures with very inhomogeneous doping profiles and various pn-junctions that cause thermal leakage currents. The latter are believed to falsify the slope of the T-dependence. This effect seems to be more pronounced in the case of electrons than in the case of holes. Another reason is the Hall factor as function of doping and temperature. We used theoretical results based on first-principle calculations instead of constant values. However, for the heavily doped samples the strong T-dependence of the Hall factor produces a considerable misfit to the theoretical drift mobility which wouldn't occur with a weakly T-dependent Hall factor.

Acknowledgment

This work is based on the excellent high-temperature measurements performed by Dr. Norbert Felber and Dr. Wladyslaw Grabinski. Andreas Wettstein implemented modifications of the mobility model into the DESSIS$_{-\mathrm{ISE}}$ source code. Dr. Christoph Jungemann (University of Bremen) calculated the Hall factors as function of doping and temperature. Marina Valdinoci (University of Bologna) provided doping profiles and experimental data. I'm also grateful to Stephan Mettler (Bosch) for his interest and for discussions.

References

[1] A. Schenk, "Unified Bulk Mobility for Low- and High-Field Transport in Silicon," *J. Appl. Phys.*, vol. 79, no. 2, pp. 814–34, 1996.

[2] C. Lombardi, S. Manzini, A. Saporito, and M. Vanzi, "A Physically Based Mobility Model for Numerical Simulation of Nonplanar Devices," *IEEE Trans. on CAD*, vol. 7, no. 11, pp. 1164–71, 1988.

[3] A. Schenk, *Advanced Physical Models for Silicon Device Simulation*. Computational Microelectronics, New York: Springer-Verlag, 1998.

[4] G. Masetti, M. Severi, and S. Solmi, "Modelling of Carrier Mobility Against Carrier Concentration in Arsenic-, Phosphorus- and Boron-Doped Silicon," *IEEE Trans. Electron Devices*, vol. ED-30, pp. 764–69, 1983.